Available online at www.sciencedirect.com

ScienceDirect

Ceramics International 40 (2014) 4225–4229

CERAMICS INTERNATIONAL

www.elsevier.com/locate/ceramint

Effect of magnesium content on structure and dielectric properties of cubic bismuth magnesium niobate pyrochlores

Libin Gao*, Shuwen Jiang, Ruguan Li, Bin Li, Yanrong Li

State Key Laboratory of Electronic Thin Films and Integrated Devices, University of Electronic Science and Technology of China, Chengdu 610054, China

Received 8 August 2013; received in revised form 16 August 2013; accepted 18 August 2013
Available online 27 August 2013

Abstract

Structure and dielectric properties of cubic pyrochlore $Bi_{1.5}Mg_NNb_{2.5-N}O_{8.5-1.5N}$ (BMN) compositions with $N=0.6$–1.3 have been studied. X-ray diffraction (XRD), infrared reflectivity spectra and Raman spectra were employed to analyze the crystal structures and phonon vibration modes of BMN compositions. The vibration spectra were sensitive to the content of Mg^{2+} ions, which is caused by the randomness of Mg^{2+} ions partially filling both the cubic pyrochlore A and B sites. The intensity of A3O stretching vibrations became stronger with increasing Mg^{2+} content, but B3O stretching vibrations were quite opposite. With the increase of Mg^{2+} content, the dielectric constant and loss tangent both increased. Temperature dependent dielectric constant was observed in the samples with $N>0.8$. The tendency of the dielectric constant with the increasing temperature showed a quick drop in the samples with higher Mg^{2+} content, which seems to be associated with the disorder in the A_2O' network.

Keywords: Cubic pyrochlore; Dielectric; Crystal structure; Raman spectroscopy

1. Introduction

With the rapid development of communication technologies, especially mobile communication systems, the miniaturization of devices are desired. Dielectric films with high permittivity have been investigated for reducing the size of microelectronic devices, such as integrated high-density storage devices, decoupling capacitors, and novel electric-field tunable devices. For such applications, materials with low dielectric loss and low temperature coefficient of capacitance (TCC) are also required. Recently, Bismuth-based pyrochlores have received considerable attention due to their moderately high permittivity, small dielectric loss, and good temperature stability [1–5]. As a member of the bismuth-based pyrochlores, the $Bi_{1.5}MgNb_{1.5}O_7$ thin films have been reported with medium dielectric constant (~86–179) [6–10], relatively low dielectric loss (~0.0018) [6], a modest TCC (−550 ppm/°C), and especially dielectric tunability of 50% at bias field of 1.5 MV/cm [8], which make the $Bi_{1.5}MgNb_{1.5}O_7$ thin films attractive candidates for high frequency voltage tunable filters and phase shifter applications.

The cubic pyrochlores have a complicated structure, and many researches show that the dielectric properties of cubic pyrochlore $Bi_{1.5}MgNb_{1.5}O_7$ have a correlation with its structure [7–10]. The cubic pyrochlore, space group Fd3m, has a formula of $B_2O_6 \cdot A_2O'$ with different types of oxygen ions [11,12]. The arrangement consists of a three dimensional network of B_2O_6 octahedra linked with an A_2O' tetrahedra in the interstices. In Bi_2O_3–MgO–Nb_2O_5 system, it can be predicted that the Bi^{3+} ions are inclined to occupy the larger A sites, the Nb^{5+} ions tend to occupy the smaller B sites, while the Mg^{2+} ions can occupy both A and B sites due to the medium radius of Mg^{2+} ions according to the crystal chemistry principle [10,13]. In this case, the substitution of randomly displacive ions makes the system in a disordered state. The correlative researches showed that the dielectric properties of bismuth based pyrochlores are closely related to this disorder [6,14,15].

In order to investigate the correlation of dielectric properties with the random structure, the cubic pyrochlore bismuth–magnesium niobate ceramics with different compositions of

*Corresponding author. Tel.: +86 288 320 0578; fax: +86 288 320 2569.
E-mail addresses: biner167@sina.com, biner167@hotmail.com (L. Gao).

0272-8842/$ - see front matter © 2013 Elsevier Ltd and Techna Group S.r.l. All rights reserved.
http://dx.doi.org/10.1016/j.ceramint.2013.08.085

$Bi_{1.5}Mg_NNb_{2.5-N}O_{8.5-1.5N}$ (BMN, N=0.6–1.3) were performed in this work. The detailed phonon vibration modes in BMN compositions were described. Their crystal structures and dielectric properties were also systematically investigated.

2. Experimental procedure

The ceramics of $Bi_{1.5}Mg_NNb_{2.5-N}O_{8.5-1.5N}$ (N=0.6–1.3) were synthesized by conventional powder processing technique. The raw materials were Bi_2O_3, MgO and Nb_2O_5 powders with purity of >99.5%. The mixture materials in stoichiometry were mixed in alcohol media with planetary ball mill for 7 h, then dried and calcined at 950 °C for 2 h. After remilling, the powders were dried and sintered into discs with diameter of 10 mm and thickness of 1 mm at 1150 °C for 2 h.

The crystalline phase of samples was characterized by X-ray diffraction (XRD, Bede D1) instrument. Room temperature infrared reflectivity spectra were obtained by a Fourier transform spectrometer (Bruker Tensor 27) in the frequency range of 200–4000 cm^{-1}. Raman spectra in the range of 50–1000 cm^{-1} were recorded on FT-Raman spectrometer (Jobin Yvon HR800). For dielectric measurements, low-fire silver electrodes were used. The dielectric measurements were performed on an Agilent 4284A precision impedance analyzer with a 500 mV test oscillation voltage.

3. Results and discussion

The XRD patterns of BMN ceramics as a function of Mg^{2+} content are shown in Fig. 1. The main phases were indexed to cubic pyrochlore with the space group Fd3m, but secondary phases were detected in the samples with Mg^{2+} concentration greater or less than that of the sample with N=1.0. The secondary phases at N=0.6 were indexed to be $Bi_{1.7}Nb_{0.3}O_{3.3}$ and $MgNb_2O_6$ phases. These secondary phases were gradually decreasing with the increase of Mg^{2+} concentration. In bulk ceramics prepared by the mixed oxide route, Bi_2O_3 and Nb_2O_5 reacted first to form Bi_2O_3–Nb_2O_5 compounds, while the formation of pyrochlore phase occurred through the reaction of bismuth niobate compounds with MgO [16]. The secondary bismuth niobate phase and magnesium niobate phase coexisted in the ceramics with $N<1.0$ was due to the lack of Mg^{2+} ions, which may result in the cubic pyrochlore structure cannot be fully formed in stoichiometry. However, the existence of the $Mg_4Nb_2O_9$ phase in the samples with $N>1.0$ was a consequence of the excessive Mg^{2+} ions in the form of magnesium niobate.

Fig. 2 shows the variation of the lattice constant with the composition N. The lattice constant showed a strong dependence on Mg^{2+} concentration. That is, lattice constant increased with the increasing of Mg^{2+} concentration until the N=1, then decreased with the excess Mg^{2+} concentration. The ionic radius of Bi^{3+} and Nb^{5+} is 0.103 and 0.64 Å, respectively. This indicates that the average radius of B-sites is larger than that of A-sites. The Mg^{2+} ions randomly occupy B sites to form homogenous solid solution phases may be the reason for the increase of lattice constant in the samples with $N<1.0$. However, the decrease of lattice constant with excess Mg^{2+} concentration can be correlated with the A sites.

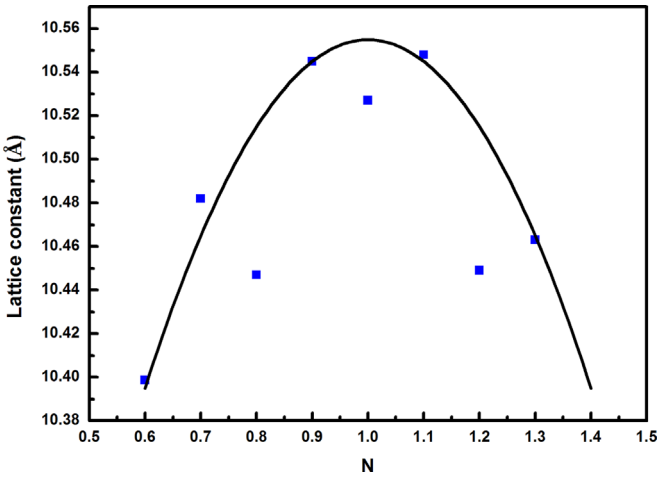

Fig. 2. Lattice constants of BMN ceramics as a function of Mg^{2+} content.

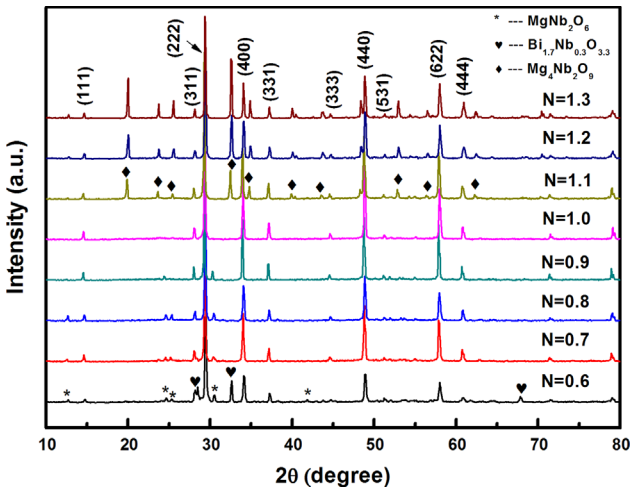

Fig. 1. XRD patterns for $Bi_{1.5}Mg_NNb_{2.5-N}O_{8.5-1.5N}$ ceramics.

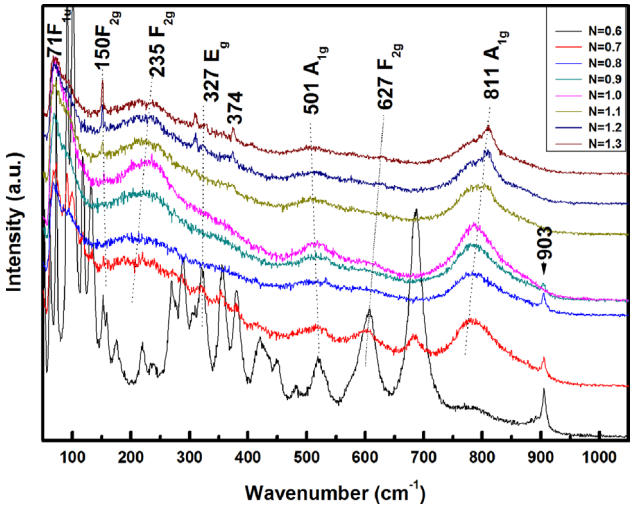

Fig. 3. Raman spectra of $Bi_{1.5}Mg_NNb_{2.5-N}O_{8.5-1.5N}$ ceramics.

Raman spectroscopy is concerned with the change of frequency when light is scattered by molecules. The Raman shifts correspond to vibrational or rotational transitions of the scattering molecule. There are six Raman active modes ($A1g+E_g+4F_{2g}$) in ideal pyrochlore structure according to group theory [17–19]. Raman spectra of BMN ceramics as a function of Mg^{2+} content in the range 100–1000 cm^{-1} are shown in Fig. 3. The sample with $N=0.6$ showed the disordered variation of Raman modes, which was caused by secondary bismuth niobate phases according to XRD analyses. The mixed phases increased the number of Raman active modes.

The Raman spectrum of BMN were best fit by eight Lorentzian oscillators located around 71, 150, 235, 327, 501, 627, 811, and 903 cm^{-1} as shown in Table 1. The Lorentzian oscillator parameters were determined by the sum of Lorentzian functions: $\sum A_j/[1+4(\omega-\omega_{oj})^2/\gamma_j^2]$, where A_j is a band maximum, ω_{oj} is a center frequency, and γ_j is a band width [20]. In pyrochlores, the modes below 300 cm^{-1} are due to the A_2O' network with the values of stretching constant range from 0.12 to 0.35 N cm^{-1}. However, only the modes at high frequencies are attributed to the B3O stretching modes with the high values of the stretching constant between 1.3 and 1.5 Ncm^{-1} [18,19]. In BMN systems, Mg^{2+} ions partially occupy both A and B sites, therefore the A–O bonds include Bi–O and Mg–O bonds while B–O bonds include Nb–O and Mg–O bonds. Calculated according to the charge–mass general relationship:

$$\frac{\sqrt{[q_{Mg}/m_{Mg}]}}{\sqrt{[q_{Bi}/m_{Bi}]}} = 2.4 \quad (1)$$

$$\frac{\sqrt{[q_{Mg}/m_{Mg}]}}{\sqrt{[q_{Nb}/m_{nb}]}} = 1.24 \quad (2)$$

The charge–mass ratio of the Mg^{2+} ions is greater than that of Bi^{3+} ions or Nb^{5+} ions. Thus, the bands around 150 cm^{-1} are suggested to be attributed to the Mg3O stretching modes, while the ones around 235 cm^{-1} are attributed to the Bi3O stretching modes. Similarly the band around 627 cm^{-1} and 811 cm^{-1} are related to the Mg3O stretching modes in B site and Nb3O stretching modes, respectively [12,13].

The lowest frequency around 70 cm^{-1} exhibits couplings of the O′–A3O′ bending modes, which has also been observed previously in $Bi_{1.5}MgNb_{1.5}O_7$ [20]. The A_2O' network is perturbed: A cations and O′ may be displaced from their ideal positions, which result in a large variation in the A3O bonds lengths and chemical environment. This fact can explain the observation of low frequency modes [18]. However, the band around 327 cm^{-1} and 501 cm^{-1} may correspond to the O3B3O bond bending.

The band at 903 cm^{-1} were observed in the samples with $N<1$, which deems as A_{1g} mode and corresponds to the breathing mode of the O octahedra [12,21,22]. This band intensity decreased with the increase of Mg^{2+} content. In addition, the 150 cm^{-1} band was found in the samples with $N\geq 1$ and the intensity increased with the increase of Mg^{2+} content. According to the Raman active mode assignment in Table 1, all of these above indicate that the Mg^{2+} ions are inclined to occupy B sites first and then enter A sites after the B sites are fully occupied. The Raman bands showed some shifts to red or blue directions as shown in Fig. 3. This is due to the difference in force constants of the A3O, A3O′, and B3O vibrational modes, which is caused by the cation ionic radius of A and B sites [23]. A relationship between the frequency of the A_{1g} vibrational band and B ion radius in pyrochlore oxides were previously reported [24]. With the same A ion, the larger the B ion radius the higher the A_{1g} vibrational band. The A_{1g} vibration increased from 782 to 811 cm^{-1}, which agree with the more Mg^{2+} ions in the B sites. However, the A_{1g} mode associated with O3B3O bond bending decreased from 516 to 501 cm^{-1}, indicating the excess Mg^{2+} ions were not in the B sites anymore. While, the F_{2g} mode around 150 and 235 cm^{-1} confirmed the excess Mg^{2+} ions entered the A sites.

The infrared reflectivity spectra of the investigated BMN compositions in the range 400–1500 cm^{-1} at room temperature are shown in Fig. 4. A dramatic change appeared in the samples with $N>1$. The intensity of the vibration at 483 cm^{-1}, 556 cm^{-1} and 639 cm^{-1} increased sharply. The vibrations at 483 cm^{-1} are assigned to A3O′ stretch mode, while the 556 cm^{-1} and 639 cm^{-1} bands are related to B3O stretch mode [25,26]. The increase of the A3O′ stretch mode with increasing Mg^{2+} content indicating more and more Mg^{2+} ions entered A

Table 1
Summary of Raman active frequencies and mode assignment.

Mode assignment	Species	Resonant frequency ω (cm^{-1})						
		$N=0.7$	$N=0.8$	$N=0.9$	$N=1.0$	$N=1.1$	$N=1.2$	$N=1.3$
O′3A3O′ bond bending	F_{1u}	66	66	68	70	70	71	71
A3O stretching	F_{2g}	–	–	–	154	151	150	150
A3O stretching	F_{2g}	207	209	218	223	228	231	235
O3B3O bond bending	E_g	318	–	–	–	326	326	327
O3B3O bond bending	A_{1g}	516	510	511	510	508	506	501
B3O stretching	F_{2g}	602	–	–	614	619	622	627
B3O stretching	A_{1g}	782	782	783	784	799	809	811
B3O stretching	A_{1g}	905	904	903	–	–	–	–

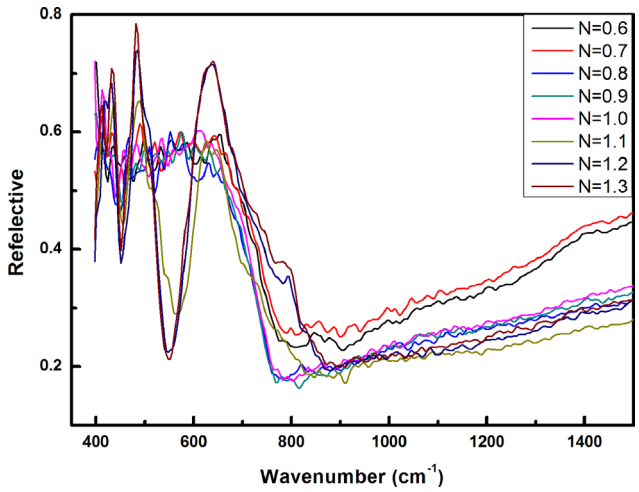

Fig. 4. Infrared reflectivity spectra of $Bi_{1.5}Mg_NNb_{2.5-N}O_{8.5-1.5N}$ ceramics.

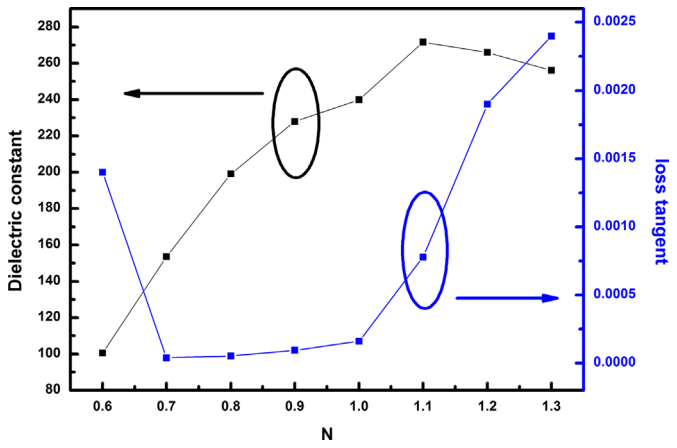

Fig. 5. Dielectric properties of $Bi_{1.5}Mg_NNb_{2.5-N}O_{8.5-1.5N}$, measured at 1 MHz with 500 mV oscillation at room temperature.

sites. While, the sharp increase of the B3O stretch mode in the sample with $N>1$ is attributed to the ordered phase with antiphase tilt of the oxygen octahedra caused by the excess Mg^{2+} ions. Thus, the phase transformation results in the modification of the polar modes of the lattice vibration [22,27].

Fig. 5 presents the room temperature dielectric properties of the samples versus the compositions of the specimens. It can be seen that the dielectric behavior varies drastically with the amount of the Mg^{2+} content. The dielectric constant increased with the increase of Mg^{2+} concentration and reached the highest value at $N=1.1$, then decreased slightly with the higher Mg^{2+} content. Dielectric properties were usually proportional to the polarizability of the constituents. Thus, the substitution of Nb^{5+} (ionic radius 0.64 Å) by larger polarizability of Mg^{2+} (ionic radius 0.66 Å) can increase the polarizability in the system, which was also evidenced by infrared reflectivity spectra. The dielectric constant decreased in the samples with $N>1.1$ may be related to the increasing secondary phase of $Mg_4Nb_2O_9$ which have a lower dielectric constant ($\sim$12.8). Another possible reason for the decrease of dielectric constant is the changes of lattice parameters [28,29]. The lattice constants showed an upward tendency with the increase of Mg^{2+} concentration, but decreased after $N>1.1$ as shown in Fig. 2.

All of the samples exhibited low dielectric loss values shown in Fig. 5. It is found that the dielectric loss increased with Mg^{2+} content except for $N=0.6$. The dielectric loss was a little large at $N=0.6$, which may be due to its multiphase structure. When $N=0.7$, the dielectric loss of the sample sharply decreased to smaller values, stayed approximately 0.0001 up to $N=1.0$ and then gradually increased with the Mg^{2+} content. Because the increase of disorder in the system allows the phonon–phonon interactions and thereby opens up many loss mechanisms [22,30]. Hopping of oxygen ion is also a possible reason for the increase of dielectric loss. These defects will absorb the photons by generating acoustic phonons, which results in higher dielectric loss.

The dielectric constant as a function of temperature for BMN ceramics is shown in Fig. 6. The dielectric constant showed no change in the samples with $N=0.7$. With the

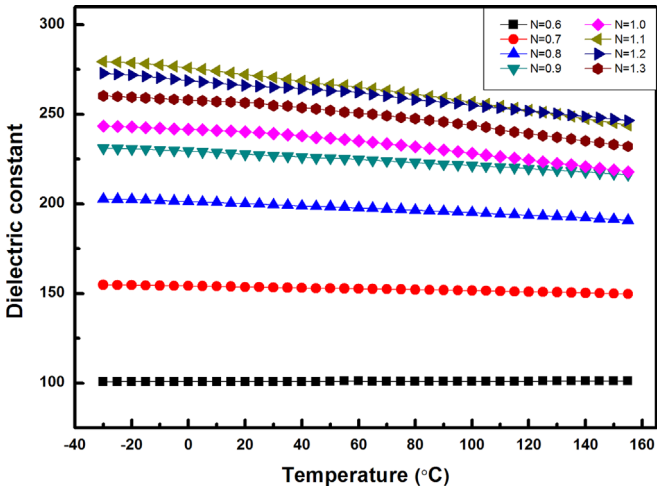

Fig. 6. The temperature dependence of dielectric constants of BMN ceramics at 1 MHz.

increase of N value, the dielectric constant dropped quickly with temperature. In general, the temperature dependence of dielectric constant may be related to polarization. This can be explained by the disorder in the A_2O' network. From the studies by Raman spectra and infrared reflectivity spectra, the additional A3O vibration modes were found in the samples ($N>1$) with high Mg^{2+} content, and their vibration intensities increased with Mg^{2+} content. This indicates that the A3O coordination environment is significantly more disordered, and the change in A_2O' network would make the polarization easier in the samples with higher Mg^{2+} concentration. Therefore, the dielectric constant of Mg^{2+}-rich samples appeared to be sensitive to temperature.

4. Conclusion

The microstructures and dielectric properties of $Bi_{1.5}Mg_NNb_{2.5-N}O_{8.5-1.5N}$ (with $N=0.6$–1.3) ceramics were investigated. The pure single cubic pyrochlore structure was found in the sample with $N=1.0$ by XRD. The Raman vibration spectra revealed that

the Mg^{2+} ions occupied B sites first and then entered A sites after the B sites were fully occupied. The microstructure significantly affected the dielectric properties of the samples. It was found that the dielectric constant and dielectric loss of samples increased with the Mg^{2+} content, but the dielectric constant showed a slight decrease when $N > 1.1$. This may result from the polarizability variation and structure disorder caused by the change of Mg^{2+} content, which was verified using Raman and infrared reflectivity spectra. The dielectric constant was nearly temperature independent at lower Mg^{2+} content ($N < 0.8$), but then it showed a tendency to decrease with the increasing temperature at higher Mg^{2+} content, which was found to be related to the disorder in the A sites.

Acknowledgments

The authors would like to thank the support from the National Natural Science Foundation of China, Grant no. 50972024.

References

[1] J.W. Lu, S. Stemmer, Effect of magnesium content on structure and dielectric properties in cubic bismuth magnesium niobate pyrochlores, Applied Physics Letters 83 (2003) 2411–2413.
[2] Y.C. Lee, Y.P. Hong, D.M. Kim, K.H. Ko, Very high tunable inter-digital capacitor using bismuth zinc niobate thin-film dielectric for microwave applications, Electrics Letters 42 (15) (2006) 851–853.
[3] W. Ren, S. Trolier-Mckinstry, C.A. Randall, T.R. Shrout, Bismuth zinc niobate pyrochlore dielectric thin films for capacitive applications, Journal of Applied Physics 89 (2001) 767–774.
[4] M.C. Wu, S. Kamba, V. Bovtun, W.F. Su, Comparison of microwave dielectric behaviour between $Bi_{1.5}Zn_{0.92}Nb_{1.5}O_{6.92}$ and $Bi_{1.5}ZnNb_{1.5}O_7$, Journal of the European Ceramic Society 26 (2005) 1889–1893.
[5] C. Ang, Z. Yu, H.J. Youn, C.A. Randall, A.S. Bhalla, L.E. Cross, J. Nino, M. Lanagan, Low-temperature dielectric relaxation in the pyrochlore $(Bi_{3/4}Zn_{1/4})_2(Zn_{1/4}Ta_{3/4})_2O_7$ compound, Applied Physics Letters 80 (2002) 4807–4809.
[6] S.W. Jiang, Y.R. Li, R.G. Li, N.D. Xiong, L.F. Tan, X.Z. Liu, B.W. Tao, Dielectric properties and tunability of cubic pyrochlore $Bi_{1.5}MgNb_{1.5}O_7$ thin films, Applied Physics Letters 94 (2009) 162908.
[7] J.K. Ahn, N.D. Cuong, S.G. Yoon, C.S. Kim, Structure and dielectric properties of $Bi_{1.5}Mg_{1.0}Nb_{1.5}O_7$ thin films deposited on $Pt/TiO_2/SiO_2/Si$ substrates by rf-magnetron sputtering, Journal of Vacuum Science and Technology B 26 (4) (2008) 1277–1280.
[8] L.B. Gao, S.W. Jiang, R.G. Li, B. Li, Y.R. Li, Structure and dielectric properties of sputtered bismuth magnesium niobate thin films, Thin Solid Films 520 (2012) 6295–6298.
[9] L.X. Li, X.Y. Zhang, L.J. Ji, P.F. Ning, Q.W. Liao, Dielectric properties and electric behaviors of tunable $Bi_{1.5}MgNb_{1.5}O_7$ thin films, Ceramics International 38 (2012) 3541–3545.
[10] S.W. Jiang, Y.R. Li, R.G. Li, L.F. Tan, N.D. Xiong, Structure and Dielectric properties of $Bi_{1.5}MgNb_{1.5}O_7$ thin films sputtered on Pt-coated sapphire substrates, Ferroelectrics 387 (2009) 1–7.
[11] M.A. Subramanian, G. Aravamudan, G.V. Subba Rao, Oxide pyrochlores —a review, Progress in Solid State Chemistry 15 (2) (1983) 55–143.
[12] H. Nyman, S. Andersson, B.G. Hyde, M. OKeeffe, The pyrochlore structure and its relatives, Journal of Solid State Chemistry 26 (1978) 123–131.
[13] H. Wang, H.L. Du, X. Yao, Structural study of Bi_2O_3–ZnO–Nb_2O_5 based pyrochlores, Materials Science and Engineering B 99 (2003) 20–25.
[14] R.A.M. Osman, A.R. West, Electrical characterization and equivalent circuit analysis of $(Bi_{1.5}Zn_{0.5})$ $(Nb_{0.5}Ti_{1.5})$ O_7 pyrochlore, Journal of Applied Physics 109 (2011) 074106.
[15] B.B. Hinojosa, A. Asthagiri, J.C. Nino, Capturing dynamic cation hopping in cubic pyrochlores, Applied Physics Letters 99 (2011) 082903.
[16] X.L. Wang, H. Wang, X. Yao, Structure, phase transformations, and dielectric properties of pyrochlores containing bismuth, Journal of the American Ceramic Society 80 (1997) 2745–2748.
[17] RA. McCauley, Infrared-absorption characteristics of the pyrochlore structure, Journal of the Optical Society of America 63 (1973) 721–725.
[18] M.T. Vandenborre, E. Husson, Comparison of the force field in various pyrochlore families. Phases presenting structural defects, Journal of Solid State Chemistry 53 (1984) 253–259.
[19] M.T. Vandenborre, E. Husson, J.P. Chatry, D. Michel, Rare-earth titanates and stannates of pyrochlore structure; vibrational spectra and force fields, Journal of Raman Spectroscopy 14 (2) (1983) 63–73.
[20] D.J. Arenas, L.V. Gasparov, W. Qiu, J.C. Nino, C.H. Patterson, Raman study of phonon modes in bismuth pyrochlores, Physical Review B 82 (2010) 214302.
[21] S. Kamba, H. Hughes, D. Noujni, S. Surendran, R.C. Pullar, P. Samoukhina, J. Petzelt, R. Freer, N.M. Alford, D.M. Iddles, Relationship between microwave and lattice vibration properties in $Ba(Zn_{1/3}Nb_{2/3})O_3$-based microwave dielectric ceramics, Journal of Physics D: Applied Physics 37 (2004) 1980–1986.
[22] F. Shi, H. Dong, Correlation of crystal structure, dielectric properties and lattice vibration spectra of $(Ba_{1-x}Sr_x)$ $(Zn_{1/3}Nb_{2/3})O_3$ solid solutions, Dalton Transactions 40 (2011) 6659–6667.
[23] K. Sudheendran, K.C. James Raju, M.K. Singh, R.S. Katiyar, Microwave dielectric and Raman scattering studies on bismuth zinc niobate thin films, Journal of Applied Physics 104 (2008) 104104.
[24] F.W. Poulsen, M. Glerup, P. Holtappels, Raman spectra and defect chemistry modeling of conductive pyrochlore oxides, Solid State Ionics 135 (2000) 595–602.
[25] H.L. Du, X. Yao, L. Zhang, Structure, IR spectra and dielectric properties of Bi_2O_3–ZnO–SnO_2–Nb_2O_5 quarternary pyrochlore, Ceramics International 28 (2002) 231–234.
[26] J.C. Nino, M.T. Lanagan, C.A. Randall, S. Kamba, Correlation between infrared phonon modes and dielectric relaxation in Bi_2O_3–ZnO–Nb_2O_5 cubic pyrochlore, Applied Physics Letters 81 (2002) 4404–4406.
[27] T. Nagai, M. Sugaiyama, M. Sando, Anoumaly in the infrared active phonon modes and its relationship to the dielectric constant of $(Ba_{1-x}Sr_x)$ $(Mg_{1/3}Ta_{2/3})O_3$ compound,, Japanese Journal of Applied Physics 35 (1996) 5163–5167.
[28] Y. Hu, C.L. Huang, Structure characterization of Bi–Zn–Nb–O cubic pyrochlores, Ceramics International 30 (2004) 2241–2246.
[29] K. Sudheendran, K.C. James Raju, Influence of post deposition anneaing process on the optical and microwave dielectric properties of $Bi_{1.5}Zn_{1.0}Nb_{1.5}O_7$ thin films, Integrated Ferroelectrics 119 (2010) 89–95.
[30] D.A. Tenne, A. Soukiassian, X.X. Xi, H. Choosciwan, R. Guo, A.S. Bhalla, Lattice dynamics in $Ba_xSr_{1-x}TiO_3$ single crystals: a Raman study, Physics Review B 70 (2004) 174302.